An Image Rejection Down Conversion Mixer Architecture

*,**Nam-Soo Kim, *Jung-Ki Choi, *Shin-Chol Kim,*Sang-Gug Lee, **Chan-Gu Lee, **Hae-Won Jung, and **Hyun-Kyu Yu,
Information and Communication University (ICU),
P.O. Box 77, Yusong, Taejoen 305-600, Korea
Phone : +82-42-866-6203 Fax : +82-42-866-6227 , kns2395@icu.ac.kr ,
**Electronics and Telecommunications Research Institute (ETRI),
161 Kajong-dong, Yusong, Taejoen 305-350, Korea

Abstract: An image rejection down-conversion mixer architecture is presented which does not require low-pass filters. The image rejection performance of conventional architectures, the Hartley and Weaver, are analyzed as a function of phase and gain mismatches and compared with the proposed architecture. The proposed architecture that adopts double poly-phase filter at the front and back of mixer shows better performance due to the inherent compensation characteristics for the mismatch signal.

Keywords
Image Rejection, Mixer, Down Conversion

I. Introduction

In the last few years, the endeavor for higher level integration of RF ICs has been the pressing interest of semiconductor industry [1][2][3][4][5]. However, the off-chip components, especially the band-pass filters, made them difficult. Among the off-chip components, the image rejection filter (IR filter) is one of the key external components. There have been various efforts to eliminate IR filter from the radio receiver, and the image rejection mixer has been the most promising solution [6][7][8].

There are two commonly known image rejection mixer architectures; Hartley and Weaver. Fig.1 shows the Hartley architecture, which is known to be sensitive to the mismatch in quadrature LO (Local Oscillator) signal as well as the 90° phase shift network [9]. Furthermore, this architecture requires low-pass filters with relatively high Q.

Figure 2 shows the Weaver architecture that consists of two mixer stages and the low-pass filters. This architecture requires two LO signals as shown in Fig. 2.

The Weaver architecture eliminates the dependencies of the image rejection characteristics on the mismatches in the 90° phase shift network, but still requires the low-pass filters, has the second image problem [9][10], and contains mismatches problems of the two LO quadrature generators.

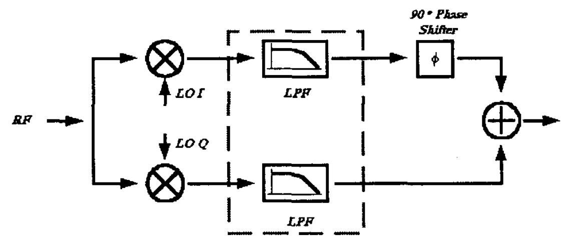

Fig. 1 Hartley Image Rejection Architecture

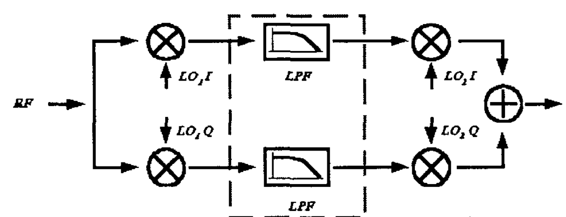

Fig. 2 Weaver Image Rejection Architecture

II. Proposed Image Rejection Mixer

Fig. 3 shows the block diagram of proposed image rejection mixer architecture. This architecture contains four mixer cells, two poly-phase filters, and the summation/subtraction stages, but no low-pass filters

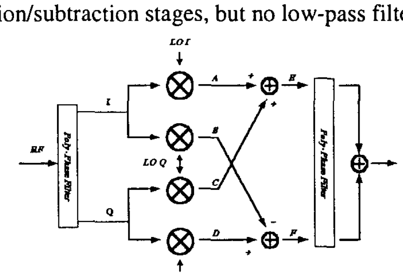

Fig. 3 The proposed Image Rejection Mixer Architecture

To analyze the proposed architecture, suppose the input signal is given by

$$RF = A_{rf}\cos(\omega_{rf}\cdot t) + A_{im}\cos(\omega_{im}\cdot t) \qquad eq(1)$$

where the first term represents desired channel and the second term the image. A_{rf} and A_{im} represent amplitudes of desired signal and that of image, respectively. ω_{rf} and ω_{im} represent frequencies of desired signal and that of image, respectively. If we assume that LO in-phase and quadrature-phase signals can be expressed as

$$LO_I = A_{lo}\cos(\omega_{lo}t) \qquad eq(2-1)$$
$$LO_Q = A_{lo}\sin(\omega_{lo}t) \qquad eq(2-2)$$

where LO_I and LO_Q represent the fundamental components of in-phase and quadrature-phase signals of LO. Neglecting the frequency conversion factors and focusing only the frequency components of mixed signal, the outputs at node A-D can be given by

$$A = \frac{1}{2}[A_{rf}A_{lo}\cos(\omega_{rf}-\omega_{lo})t + A_{im}A_{lo}\cos(\omega_{lo}-\omega_{im})t + A_{rf}A_{lo}\cos(\omega_{rf}+\omega_{lo})t + A_{im}A_{lo}\cos(\omega_{lo}+\omega_{im})t] \quad eq(3-1)$$

$$B = \frac{1}{2}[-A_{rf}A_{lo}\sin(\omega_{rf}-\omega_{lo})t + A_{im}A_{lo}\sin(\omega_{lo}-\omega_{im})t + A_{rf}A_{lo}\sin(\omega_{rf}+\omega_{lo})t + A_{im}A_{lo}\sin(\omega_{lo}+\omega_{im})t] \quad eq(3-2)$$

$$C = \frac{1}{2}[A_{rf}A_{lo}\cos(\omega_{rf}-\omega_{lo})t + A_{im}A_{lo}\cos(\omega_{lo}-\omega_{im})t - A_{rf}A_{lo}\cos(\omega_{rf}+\omega_{lo})t - A_{im}A_{lo}\cos(\omega_{lo}+\omega_{im})t] \quad eq(3-3)$$

$$D = \frac{1}{2}[A_{rf}A_{lo}\sin(\omega_{rf}-\omega_{lo})t - A_{im}A_{lo}\sin(\omega_{lo}-\omega_{im})t + A_{rf}A_{lo}\sin(\omega_{rf}+\omega_{lo})t + A_{im}A_{lo}\sin(\omega_{lo}+\omega_{im})t] \quad eq(3-4)$$

From equation (3) we see that A+C and D-B eliminate the up-converted frequency components, $\omega_{rf} + \omega_{lo}$ and $\omega_{im} + \omega_{lo}$. With the Hartley and Weaver architecture, low-pass filters are used to eliminate the up-converted components.

After summation and subtraction, the F node output is shifted by 90° and the E node output stays in-phase through poly-phase filter. The differential summation at the final output node eliminates the image signal. In this process mismatch raised from the LO quadrature generator and signal paths are compensated. Fig. 4 shows image rejection operation of the proposed architecture in frequency domain. The ash colored block represents image band and the white colored one the desired band.

III. Comparative Analysis of the Image Rejection Architectures

If the phase and gain mismatch is represented by ε and θ, respectively, and the path gain mismatch is ignored, the image rejection ratio (IRR) of Hartley architecture is given by[10]

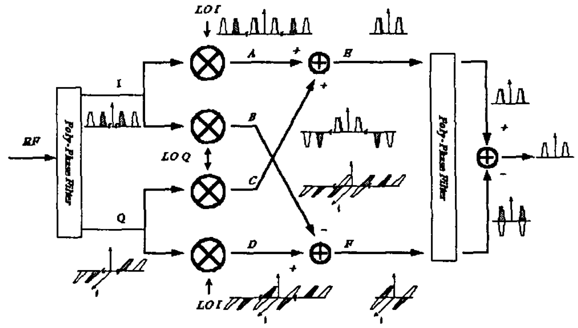

Fig. 4 Frequency domain analysis of proposed image rejection architecture

$$IRR_{Hatley} = \frac{(A_{lo}+\varepsilon)^2 - 2A_{lo}(A_{lo}+\varepsilon)\cos\theta + A_{lo}^2}{(A_{lo}+\varepsilon)^2 + 2A_{lo}(A_{lo}+\varepsilon)\cos\theta + A_{lo}^2} \qquad (4)$$

Similarly, the IRR of the Weaver architecture can be expressed by

$$IRR_{Weaver} = \frac{(A_{lo1}+\varepsilon_1)^2(A_{lo2}+\varepsilon_2)^2 - 2(A_{lo1}+\varepsilon_1)(A_{lo2}+\varepsilon_2)A_{lo1}A_{lo2}\cos(\theta_1-\theta_2) + A_{lo1}{}^2A_{lo2}}{(A_{lo1}+\varepsilon_1)^2(A_{lo2}+\varepsilon_2)^2 + 2(A_{lo1}+\varepsilon_1)(A_{lo2}+\varepsilon_2)A_{lo1}A_{lo2}\cos(\theta_1-\theta_2) + A_{lo1}{}^2A_{lo2}} \qquad (5)$$

where A_{lo1} and A_{lo2} represent amplitudes of the 1st and 2nd LO signal, respectively.

Following the approaches applied to the Hartley and Weaver architectures, the signal at the E and F node of the newly proposed image rejection mixer can be expressed as

$$A + C = \frac{1}{2}[A_{rf}A_{lo}\cos(\omega_{rf}-\omega_{lo})t + A_{im}A_{lo}\cos(\omega_{lo}-\omega_{im})t + A_{rf}(A_{lo}+\varepsilon)\cos((\omega_{rf}-\omega_{lo})t-\theta) + A_{im}(A_{lo}+\varepsilon)\cos((\omega_{lo}-\omega_{im})t+\theta)] \qquad (6)$$

$$-B + D = \frac{1}{2}[A_{rf}(A_{lo}+\varepsilon)\sin((\omega_{rf}-\omega_{lo})t-\theta) + -A_{im}(A_{lo}+\varepsilon)\sin((\omega_{lo}-\omega_{im})t+\theta) + A_{rf}A_{lo}\sin(\omega_{rf}-\omega_{lo})t - A_{im}A_{lo}\sin(\omega_{lo}-\omega_{im})t] \qquad (7)$$

Ignoring the additional mismatches of the 2nd poly-phase filter, from equation (6) and (7), the final output signal at the output of the proposed mixer contains no image signals regardless of the amount of the mismatches. The proposed architecture inherently compensates the gain and phase mismatches leading to ideally infinite IRR.

Based on equations (4) and (5), the image rejection characteristics of the Hartley and Weaver architectures are analyzed. Fig. 5-(a) and 5-(b) represent the IRR of the Hartley architecture, while 5-(c) through 5-(f) that of the Weaver. Fig. 5-(a) shows the IRR variation as a function of the phase and gain mismatch for small LO amplitude. And, Fig. 5-(b) is for the large LO amplitude. As can be seen from Fig. 5-(a) and -(b), the Hartley architecture shows

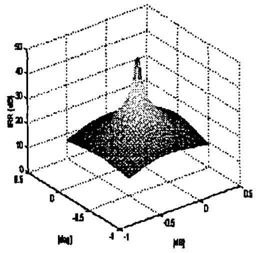

(a) Hartley, small LO amplitude.

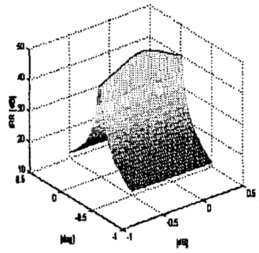

(b) Hartley, large LO amplitude.

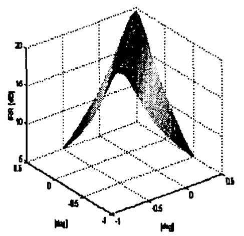

(c) Weaver, phase variation, small LO amplitude.

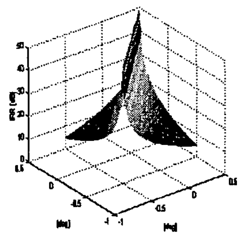

(d) Weaver, phase variation, large LO amplitude.

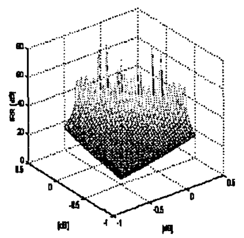

(e) Weaver, amplitude variation, small LO amplitude.

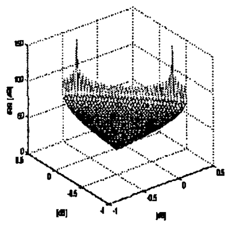

(f) Weaver, amplitude variation, large LO amplitude.

Fig. 5 IRR of Hartley and Weaver architecture as a function of phase and gain mismatches.

improvement in IRR for larger LO amplitude. Fig. 5-(c) and -(d) shows the IRR variation as a function of the mismatches in the phases of LO_1 and LO_2. Again, the larger LO amplitude helps the image rejection performance. Fig. 5-(e) and -(f) shows the IRR variation as a function of LO_1 and LO_2 gain mismatches, assuming phase mismatches are negligible. Fig. 5-(e) and -(f) shows that the IRR are less sensitive to gain mismatch, and again, the larger LO amplitude helps to improve the image rejection.

Conclusion

A new image rejection architecture is proposed and analyzed. The proposed image rejection mixer dose not require low-pass filter therefore it can be used to high IF frequency applications where the integrated low-pass filter is not feasible.

The image rejection performance of proposed architecture is analyzed and compared with the conventional Hartley and Weaver architectures and demonstrates superiority of proposed architecture.

The phase and gain mismatch dependencies of the Hartley and Weaver architectures are investigated and showed that the IRR is more sensitive to the phase mismatch, and, the larger LO amplitudes help to minimize the gain and phase mismatch effects.

Reference

[1] John R. Long and Miles A. Copeland, "A 1.9GHz Low-Voltage Silicon Bipolar Receiver Front-End for Wireless Personal Communications Systems," *IEEE J. Solid State Circuits*, vol. 30, No. 12, December 1995.

[2] Jacques C. Rudell *et al.*,"A 1.9-GHz Wide-Band IF Double Conversion CMOS Receiver for Cordless Telephone Applications," *IEEE J. Solid State Circuits*, vol. 32, No. 12, December 1997.

[3] Jan Crols and Michel S. J. Steyaert, "A Single Chip 900MHz CMOS Receiver Front-End with a High Performance Low-IF Topology," *IEEE J. Solid State Circuits*, vol. 30, No. 12, December 1995.

[4] Ahmadreza Rofougaran, Glenn Chang, *et al.*," A Single-Chip 900-MHz Spread-Spectrum Wireless Transceiver in 1- m CMOS—Part II: Receiver Design," *IEEE J. Solid State Circuits*, vol. 33, No. 4, April 1998.

[5] Behzad Razavi, "Recent Advances in RF Integrated Circuits," *IEEE Communication Magazines*, December 1997.

[6] M. Banu *et al.*, "A BiCMOS double-low-IF receiver for GSM," in *Custom Integrated Circuits Conf.*, May 1997, pp. 521–524.

[7] W. Baumberger, "A single-chip image rejecting receiver for the 2.44GHz GHz band using commercial GaAs-MESFET-technology," *IEEE J. Solid-State Circuits*, vol. 29, pp. 1244–1249, Oct. 1994.

[8] Seungwook Lee *et al.*," A 1GHz Image-Rejection Down-Converter in 0.8u CMOS Technology," *IEEE Trans. on Consumer Electronics*, vol 44, No. 2, pp. 235-239, May 1998.

[9] Behzad Razavi, "Architectures and Circuits for RF CMOS Receivers," *Proc. CICC*, pp. 393-400, 1998

[10] Behzad Razavi, " *RF Microelectronics*," Prentice Hall, 1988.